Electron degradation and yields of initial products. VII. Subexcitation electrons in gaseous and solid H_2O

M. A. Ishii, Mineo Kimura,* and Mitio Inokuti
Argonne National Laboratory, Argonne, Illinois 60439
(Received 11 December 1989)

A comparative study of electron degradation spectra and yields for various species in gaseous and solid H_2O is carred out by using the rigorous Spencer-Fano theory and the continuous-slowing-down approximation (CSDA). As input we use cross-section data given by Hayashi [in *Atomic and Molecular Data for Radiotherapy,* Proceedings of an IAEA Advisory Group Meeting, Vienna, June 1988, Report No. IAEA-TECDOC-506 (International Atomic Energy Agency, Vienna, 1989), p. 193] for the gas and by Michaud and Sanche [Phys. Rev. **36**, 4672 (1987)] for the solid. Vibrational excitation is the dominant mechanism of the slowing down of the electron in both gas and solid phases at intermediate energies of 8–2 eV. Rotational excitation for the gas and phonon excitation for the solid, which share the same origin of dynamics, are the second important mechanism. The general trends of the electron degradation spectra are similar in the two phases. However, details of the spectra differ notably from one another. Because the energy dependence of some of the cross sections is complex, the CSDA fails to reproduce even a local average of the Spencer-Fano degradation spectrum, and gives yields of various products appreciably different from those evaluated from the Spencer-Fano degradation spectrum.

I. INTRODUCTION

A series of studies[1–7] on subexcitation electrons in gases led to several important observations, which concern, for instance, the competition of the slowing down of the electron with other processes,[1,3] the validity of the continuous-slowing-down approximation (CSDA),[2,4] and structures in the entry spectrum.[5,6] A summary of these studies together with their background is seen in a review article.[7] These studies are all based on realistic cross-section data for electron collisions determined through critical review of experimental and theoretical data.

For subexcitation electrons in solids, cross-section values were virtually nonexistent until recently. Therefore the initial report by Michaud and Sanche[8,9] on this topic is noteworthy. They conducted a series of measurements on electron transmission and reflection in thin films of amorphous solid H_2O, performed an analysis of electron transport, and thereby deduced cross sections for individual scattering processes of electrons of energies 1–20 eV. The cross-section data thus determined are useful for studying various problems in the earliest stages of radiation action. Indeed, Goulet and Jay-Gerin[10] used the data in their Monte Carlo study of "electron thermalization" (which more precisely ought to be called slowing down of the electron to 0.3 eV).

The purpose of the present work is to study the moderation of subexcitation electrons in H_2O, both solid and gas. For the solid we use the cross-section values given by Michaud and Sanche.[8,9] For the gas we use mainly the cross-section values given by Hayashi,[11] who reviewed data in the literature extensively and critically to arrive at the best possible values. For analysis of the electron moderation we use the Spencer-Fano theory and the CSDA. In summary, the present study is comparative in two respects: gas versus solid and Spencer-Fano theory versus the CSDA.

II. THEORY

Full discussions of the Spencer-Fano (SF) equation and the continuous-slowing-down approximation have been given earlier.[12,13] We present here only a brief summary of the theory to provide a framework for later discussion.

A. The Spencer-Fano equation

The electron degradation spectrum $y(T)$, under stationary irradiation, satisfies the SF equation

$$nK_T y(T)+U(T)=0 , \tag{1}$$

where T is the electron kinetic energy, K_T represents the cross-section operator,[13] and n is the number density of molecules in the medium. The symbol $U(T)$ represents the spectrum of source electrons. In particular, for monoenergetic electrons with initial kinetic energy T_0, we set $U(T)=\delta(T-T_0)$ and denote the solution as $y(T_0,T)$. Once $y(T_0,T)$ is obtained, the mean yield $N_s(T_0)$ of any initial product s is calculated as

$$N_s(T_0)=n\int_0^{T_0} dT\, y(T_0,T)\sigma_s(T) , \tag{2}$$

where $\sigma_s(T)$ represents the cross section for the production of s. By the term "initial products" we mean here ions, excited states, dissociation fragments, and other molecular species that are formed *immediately following electron collisions and degradation.* This usage is different from that of radiation chemists, in which initial products

mean the species that signals the initial condition for diffusion and chemical kinetics. The initial condition here refers to much later time than electron degradation.

For the time-dependent case, i.e., when the source of the incident electrons depends on time t, the SF equation is modified. In particular, for a pulsed monoenergetic source, the *incremental* electron degradation spectrum $z(T_0,T;t)$ satisfies the equation[13]

$$\frac{1}{v_T}\frac{\partial z(T_0,T;t)}{\partial t}=nK_T z(T_0,T;t)+\delta(T_0-T)\delta(t)\ , \tag{3}$$

where v_T is the speed of an electron of energy T. The stationary degradation spectrum $y(T_0,T)$ is related to $z(T_0,T;t)$ by

$$y(T_0,T)=\int_0^\infty z(T_0,T;\lambda)d\lambda\ , \tag{4}$$

B. The continuous-slowing-down approximation

Provided (i) that there is no generation of secondary electrons, (ii) that every possible energy loss per collision is *small* compared to electron kinetic energy, and (iii) that cross sections are smooth as a function of T, then the CSDA should be a reasonable approximation. This will be seen from the following treatment.

Under assumption (i), we may express the cross-section operator as

$$K_T f(T)=\sum_s \sigma_s(T+E_s)f(T+E_s)-f(T)\sum_s \sigma_s(T)\ , \tag{5}$$

where $f(T)$ is any operand function of T, and $\sigma_s(T)$ is the cross section for a collision in which an electron of energy T suffers energy loss E_s. The sum includes all possible processes, and therefore E_s may be discrete or continuous. Assumption (ii) means that $E_s \ll T$ for every m, and therefore we may use the Taylor-series expansion to obtain

$$K_T f(T)=\sum_{j=1}^{\infty}(j!)^{-1}\left[\frac{d}{dT}\right]^j[s^{(j)}(T)f(T)]\ , \tag{6}$$

where $s^{(j)}(T)$ is the jth moment of energy loss, defined as

$$s^{(j)}T=\sum_s E_s^j\sigma_s(T)\ . \tag{7}$$

Finally, under assumption (iii) it is reasonable to expect that all but the $j=1$ term in Eq. (6) is appreciable. Thus we arrive at

$$K_T f(T)=\frac{d}{dT}[s^{(1)}(T)f(T)]\ , \tag{8}$$

which is customarily referred to as the CSDA. In other words, Eq. (8) is justified if the product $s^{(j)}(T)f(T)$ for every $j\geq 2$ is a slowly varying function of T.

Within the CSDA, Eqs. (1) and (3) can be simplified a great deal. First, the use of Eq. (8) in Eq. (1) readily leads to

$$y(T)=[ns^{(1)}(T)]^{-1}\int_T^\infty dT' U(T')\ . \tag{9}$$

This result means that the total path length of electrons is given as the total number of the source electrons divided by the stopping power $ns^{(1)}(T)$.

Second, the use of Eq. (8) in Eq. (3) leads to a partial differential equation of the first order, which is always analytically solvable, as fully discussed in Refs. 1 and 13. In summary, the partial differential equation takes a simple form

$$\left[\frac{\partial}{\partial t}+\frac{\partial}{\partial \tau}\right]s^{(1)}z(T_0,T;t)=v_T s^{(1)}\delta(T_0-T)\delta(t)\ , \tag{10}$$

where

$$\tau=\int_T^{T_0}[v_\lambda ns^{(1)}(\lambda)]^{-1}d\lambda \tag{11}$$

is a variable that is uniquely related to electron energy T. The meaning of τ is elementary from the following. Recall that the stopping power $ns^{(1)}(T)$ signifies the mean energy loss from an electron of energy T per unit path length. Therefore $v_T ns^{(1)}(T)$ signifies the mean energy loss of an electron of energy T per unit time. Consequently, τ signifies the mean time required for an electron of energy T_0 to slow down to energy T, evaluated within the CSDA. Thus we call τ the CSD time.

III. CROSS SECTIONS USED AS INPUT

A. Gas

Figure 1 shows the cross sections for gaseous H_2O as functions of electron energy T. The data are primarily based on the compilation by Hayashi,[11] and in part taken from Shyn, Cho, and Cravens,[14] Itikawa,[15] and Jain and Thompson.[16]

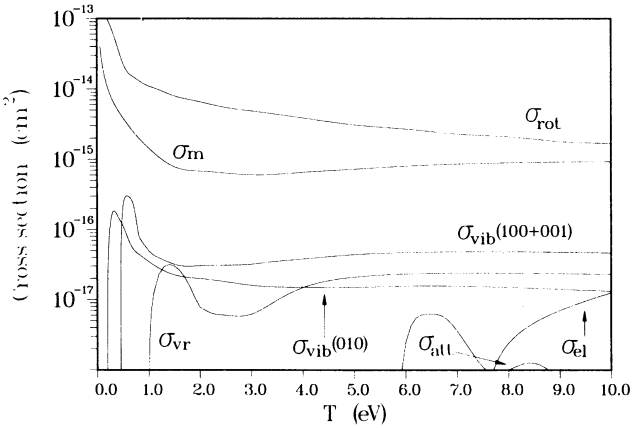

FIG. 1. Cross sections for electron collisions with gaseous H_2O as functions of electron energy T. Data are taken from Refs. 11 and 14–16. The symbol σ_m represents the momentum transfer cross section, σ_{rot} the rotational-excitation cross section (more precisely, the net cross section for net energy loss resulting from rotational excitation and deexcitation). The symbol $\sigma_{vib}(100+001)$ represents the sum of the cross sections for the excitation of the 100 and 001 vibrational modes, $\sigma_{vib}(010)$ the cross section for the excitation of the 010 vibrational mode, and σ_{vr} the sum of all the other vibrational excitations. The symbol σ_{att} represents the cross section for dissociative attachment leading to the H^- formation and σ_{el} the cross section for electronic excitation.

Vibrational excitations are grouped into three channels of appreciably differing energy losses. First, $\sigma_{100+001}$ represents the sum of the cross sections for excitation of the two stretching modes 100 and 001, with a mean threshold energy of 0.453 eV. The difference in the excitation energies for the two modes is too small to be resolved in current cross-section measurements. Second, σ_{010} represents the cross section for the excitation of the 010 mode. The values of $\sigma_{100+001}$ and σ_{010} are taken from the recent work by Shyn *et al.*[14] Finally, σ_{vr} represents the sum of cross sections for all the other kinds of vibrational excitation, and its value is less certain.

The rotational-excitation cross section σ_{rot} is based on theoretical results.[15,16] More precisely, σ_{rot} represents the cross section for net energy loss resulting from rotational excitation and deexcitation. We use the Born approximation results of Itikawa[15] at the lower energies and the close-coupling results of Jain and Thompson[16] at the higher energies.

The momentum transfer cross section σ_m is taken from Hayashi,[11] who derived it from analysis of swarm data.

The electronic-excitation cross section σ_{el} is taken also from Hayashi.[11] There are no direct experimental data for σ_{el}; its value had to be inferred from swarm data and the knowledge of other cross sections and therefore is not very certain.

The dissociative-attachment cross section σ_{att} refers to the process

$$e^- + H_2O \rightarrow H_2O^- \rightarrow H^- + OH \ . \tag{12}$$

The direct production of OH^- is negligible. However, OH^- is subsequently formed through the reaction

$$H^- + H_2O \rightarrow H_2 + OH^- \ , \tag{13}$$

as fully documented by Melton and Neece.[17,18] The same mechanism should occur in liquid and accounts for the radiation-chemical yield of unscavengeable H_2, as pointed out by Platzman.[19]

It is appropriate here to discuss briefly why the cross sections for different collision processes have different magnitudes and behave differently as functions of electron energy. The rotational-excitation cross section σ_{rot} and the momentum transfer cross section σ_m are chiefly governed by the long-range dipole interactions. Therefore their magnitudes are large, and the energy dependence is smooth. The rise of these cross sections at very low energies is also characteristic of the dipole interactions. The vibrational-excitation cross sections are smaller in general, because an electron must approach closer to the H_2O molecule to give larger impulse. The energy dependence of the vibrational-excitation cross sections is also stronger, for the same reason. In particular, the sharp energy dependence of $\sigma_{100+001}$ and σ_{010} at $T < 1$ eV and of σ_{vr} at 1 eV $< T <$ 3 eV is probably attributable to resonance processes in which an electron is temporarily bound to the H_2O molecule. The peaking of σ_{att} around 6.5 eV must be also attributable to a resonance, as is generally the case for dissociative attachment.

B. Solid

Shown in Figs. 2(a) and 2(b) are the cross sections used for our calculations. The data, published by Michaud and Sanche,[8,9] represent cross sections for thick amorphous ice films (approximately 30 layers) condensed at 14 K.

Not surprisingly, most of the known modes of excitation (i.e., electronic excitation and all intramolecular vibrational excitations) manifest themselves in the solid phase. The electronic excitation threshold must be similar to that in the gas, i.e., approximately 6.8 eV; hence the peak at 5 eV represents the dissociative attachment[9] which is lower than that in the gas due to a change of the polarization potential.

According to Michaud and Sanche,[8,9] there are two phonon modes: (i) ν_T, translational phonons, attributed

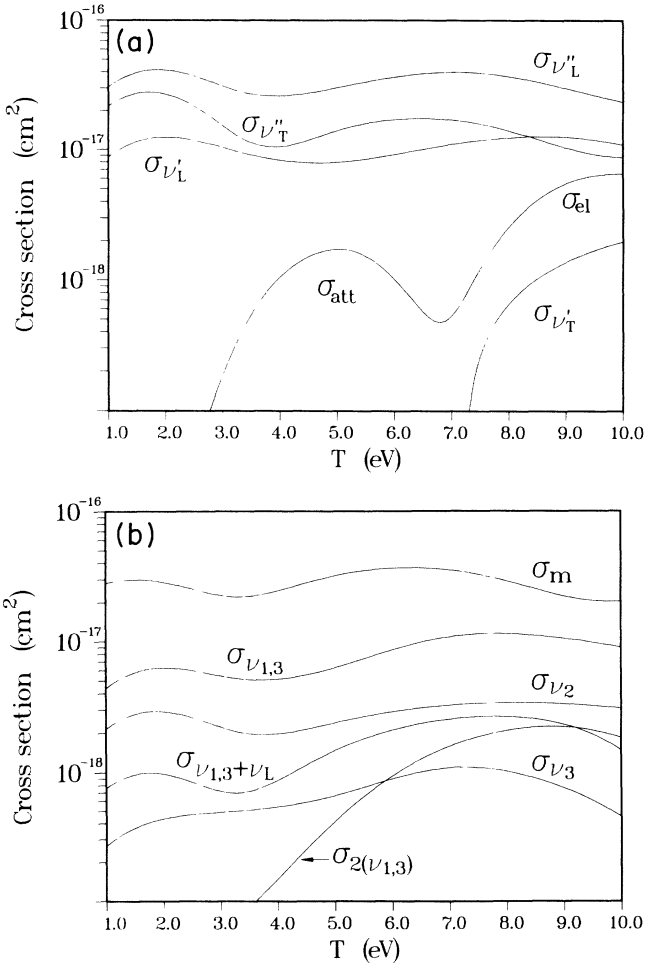

FIG. 2. Cross sections for electron collisions with solid H_2O. Data and notations are taken from Refs. 8 and 9. In (a), $\sigma_{\nu'L}$ and $\sigma_{\nu''L}$ represent the cross sections for the excitation of libration, i.e., intermolecular vibration. Symbol $\sigma_{\nu'T}$ and $\sigma_{\nu''T}$ represent the cross section for the translational-phonon excitation and σ_{el} the cross section for electronic excitation. In (b), σ_m represents the momentum transfer cross section. All the other symbols represent the cross sections for the excitation of the intramolecular vibrational modes indicated by subscripts.

to the hindered translational modes, and (ii) ν_L, librational phonons, originating from the three hindered modes of rotational excitation.

The intramolecular vibrational modes of excitation are the same as those presented for the gaseous phase; ν_2 represents the bending modes and $\nu_{1,3}$ the two stretching modes.

A remark is in order on the vibrational-excitation cross section. In general we expect some similarity in the energy dependence of the vibrational-excitation cross sections between solid and gas, because an electron must approach the molecular core closely to deliver enough momentum to excite vibration. However, as comparison of Figs. 2(a) and 2(b) with Fig. 1 indicates, the energy dependence of the vibrational-excitation cross sections in solid is qualitatively different from that in gas. Moreover, the energy dependence of the cross sections shown in Fig. 2(b) is nearly the same for all channels except for $\sigma_{2(\nu_{1,3})}$. Reasons for these aspects of the cross sections remain obscure to us. Nevertheless, we feel it worthwhile to examine the consequences of the cross sections in the electron degradation calculation as discussed below.

IV. DEGRADATION SPECTRUM

The degradation spectrum $y(T_0, T)$ will be discussed as a function of the electron energy T resulting from monoenergetic incident electrons of energy T_0. Throughout we treat a "gas" at 1 atm and 0 °C and a solid at 14 K. It is convenient to discuss the SF and the CSDA cases separately and we begin the CSDA first.

A. The CSDA analysis

1. Gas

The dashed curve in Fig. 3 represents the degradation spectrum for gaseous H_2O calculated from the CSDA. The incident energy is set at 10 eV to show the transitional behavior into the subexcitation domain. The calculation is extended down to 0.06 eV to study the role of rotational excitation.

Inspection of the results from higher energies to lower indicates the following features. (i) A marked upward trend from 10 to 7.5 eV is due to the waning effect of electronic excitation. (ii) A decrease from 7.5 to about 5.8 eV is attributable to electron attachment. (iii) A rather structureless region between 5.8 and 2 eV results from the smoothness of cross sections in this region. (iv) Below 2 eV the three distinct minima correspond to the three maxima in the vibrational-excitation cross sections σ_{vr}, $\sigma_{vib}(010)$, and $\sigma_{vib}(100+001)$. (v) Finally, a rather drastic downward trend below the lowest vibrational threshold value is attributable to rather large rotational-excitation cross sections.

Rotational excitation plays a notable role in electron degradation in gaseous H_2O. Despite the small energy loss per collision, rotational excitation accounts for over 27% of the total energy loss by degrading electrons. This arises from large cross sections resulting from dipole interactions. In contrast, rotational excitation plays a much smaller role in nonpolar molecules, e.g., nitrogen[2] and oxygen.[4] The contribution of rotational excitation to the total energy loss in H_2O is not uniform over energy but grows from about 6% at 10 eV to slightly over 53% at 1.2 eV and is higher at lower energies. This is understandable from the shape of the rotational-excitation cross section. The dominance of rotational excitation in the lower-energy region has the effect of damping other energy-loss processes. This can be seen in the weak influence of the vibrational cross-section maxima on the degradation spectra and their minor contribution to the yield, as discussed further in Sec. V.

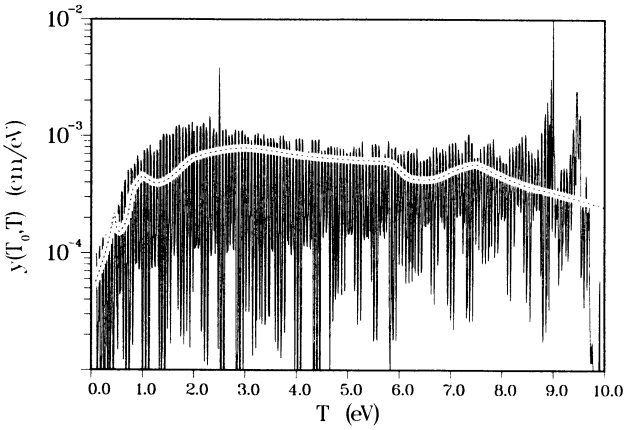

FIG. 3. Electron degradation spectrum $y(T_0, T)$ as a function of electron energy T in gaseous H_2O for the source energy $T_0 = 10$ eV. The solid curve represents the solution of the SF equation, the dashed curve the result of the CSDA, i.e., the reciprocal of the stopping power.

2. Solid

Figure 4 shows the degradation spectrum for solid H_2O as calculated from the CSDA (indicated by the dashed curve). The magnitude of the solid spectrum is lower than that of the gas spectrum in accordance with the higher density. The electronic-excitation threshold value is 7.5 eV, and the incident energy is set at 10 eV to allow comparison with gas. The calculation is terminated at 1 eV because of the absence of cross-section data. Note that the energy values are in reference to the vacuum level and must be shifted upward by about 1 eV if they are to be referenced to the bottom of the conduction band.

Attributing characteristics of the degradation spectra to data for individual cross sections is more difficult in the solid phase because of the similarities of the cross sections for different channels and the absence of one or two dominant channels. Perhaps a more insightful method of understanding this spectrum is to observe the general trends of a few of the more influential energy-loss processes: phonon modes ν_L' and ν_L'', vibrational modes $\nu_{1,3}$, and electronic excitation.

Upon going from higher energies to lower energies we observe the following features: (i) a slight dip between 10 and 8 eV, (ii) a gentle, yet complicated, upward trend ending around 3.5 eV, (iii) another depression below 3.5

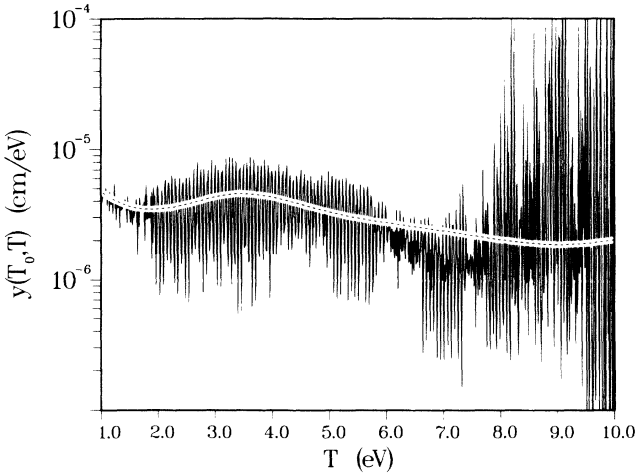

FIG. 4. Electron degradation spectrum $y(T_0,T)$ as a function of electron energy T in solid H_2O for the source energy $T_0=10$ eV. The solid curve represents the solution of the SF equation, the dashed curve the result of the CSDA, i.e., the reciprocal of the stopping power.

eV, and (iv) an upward trend at 1 eV.

The first depression results from a complex interplay of four major contributors, namely, ν_L'', $\nu_{1,3}$, $2(\nu_{1,3})$, and electronic excitation. If one looks closely at these four cross sections it is not difficult to see that this is the case.

The maxima between 3 and 4 eV followed by the dip between 1 and 3 eV are to be expected from the trends of all cross sections in this region. The phonon excitations are slightly more influential here than in the higher-energy region; this is due in part to the very small electron attachment cross section and in part to the rise in the phonon excitations compared to the reduction in other vibrational excitations.

B. Spencer-Fano analysis

Figures 3 and 4 also include degradation spectra calculated by solving the SF equation (the solid curve). As noted earlier, Fig. 3 represents the gas phase, Fig. 4 the solid phase.

First, a few generalities of the spectra are noteworthy. The entire spectrum is dominated by equally spaced discrete lines. This represents a Lewis effect,[20] which occurs at energies slightly below the incident energy because of discrete energy losses of a few collision processes.[12] The Lewis effect signifies a stochastic aspect of electron degradation and occurs in various contexts, e.g., for high-energy electrons in helium,[21,22] for electrons near an inner-shell threshold,[23] and for subexcitation electrons in nitrogen near a given source energy.[2]

At energies much lower than the source energy, the Lewis effect usually diminishes and the degradation spectrum becomes a smooth function of electron energy, because the spectrum then receives contributions from many processes of different energy losses, as seen in several examples.[2,21–23] In contrast, the degradation spectrum in H_2O continues to be structured down to very low energies. This is attributable to the importance of discrete rotational and vibrational excitations, which have rising cross sections with decreasing energies.

1. Gas

Immediately below the source energy, 10 eV, the Lewis effect is most conspicuous. The graphing resolution of Fig. 3 is insufficient to show the subtleties of the degradation spectrum because of an interplay of two processes with small energy losses, rotational excitation and momentum transfer upon elastic scattering, which compete with each other and give rise to oscillations with large magnitudes.

At lower energies we see different energy-loss processes manifesting themselves in the degradation spectrum. For example, the large increase around 9.5 eV in the spectrum is attributable to the vibrational modes (100+001). A similar effect also occurs at 9 eV.

Throughout the spectrum we notice rather discrete lines of oscillation at regularly spaced intervals. These are caused by competition among momentum transfer, rotational excitation, and (010) vibrational excitation, as seen from line spacings near the threshold energy. The changes in amplitude of these oscillations occur because the remaining channels propagate at different frequencies.

Finally, at the lower end of the spectrum the downward trend already indicated by the CSDA is present. This is a direct consequence of the large increase in the total cross sections that is chiefly due to rotational excitation. Oscillations still occur because of electrons moderating into this energy region from higher-energy regions.

2. Solid

The degradation spectrum in the solid (Fig. 4) is also dominated by the Lewis effect. Some damping of the oscillation is apparent at lower energies, where many channels contribute to the electron degradation process.

The solid phase with many channels of comparable cross sections offers a stringent test of the CSDA. As is apparent in Fig. 4, the CSDA poorly represents even the qualitative behavior of the SF solution. At intermediate energies of 6–8 eV, the CSDA greatly overestimates the degradation spectrum. At higher energies the CSDA fails to give the huge increase in the mean value of the SF solution. This leads to a severe underestimation of the total yields, as seen in Tables I and II.

Finally, we note the extreme sensitivity of the SF solution to the mesh size used for calculations. It is crucial that the mesh size be small enough to resolve momentum transfer if an accurate solution is to be obtained. We have studied the sensitivity of the SF solution to the mesh size. Details of this sensitivity study will be published elsewhere.

V. YIELD SPECTRA

We call the integrand of Eq. (2) the yield spectrum for product s. The yield spectrum represents the contribution of electrons at each energy T to the yield $N_s(T_0)$ of

that product.

Figures 5, 6(a), and 6(b) show yield spectra evaluated within the CSDA as functions of electron energy; the first figure represents the gas phase, and the latter two figures represent the solid phase. We have also evaluated the yield spectra from the solution $y(T_0,T)$ of the SF equation. The result is highly structured because $y(T_0,T)$ is highly structured, as seen in Figs. 3 and 4. For the general understanding, the yield spectra within the CSDA are more useful, although the quantitative inaccuracy of the CSDA as seen in Tables I and II must be borne in mind. (See Sec. VIII for a fuller discussion.)

A. Gas

First we discuss the spectra (Fig. 5) in gas, going from the initial energy 10 eV to lower energies. The yield spectrum of the electronic excitation is lower than those of the rotational and vibrational excitation at 10 eV and diminishes rapidly upon approach to the electronic-excitation threshold of 7.5 eV. Nevertheless, the electronic excitation dominates the total energy loss at 10 eV because of the large energy transfer per collision. Consequently, the yield spectra of all the other products are suppressed at 10 eV and gradually rise with decreasing energy down to 7.5 eV. Indeed, the yield spectra of the rotational and vibrational excitation reach maxima around there. This illustrates the appropriateness of the notion of subexcitation electrons of Platzman,[24] who pointed out consequences of the disparity in the energy-loss rate between the electronic-excitation region and the subexcitation region. This disparity is drastic in rare gases (in which subexcitation electrons lose energy solely

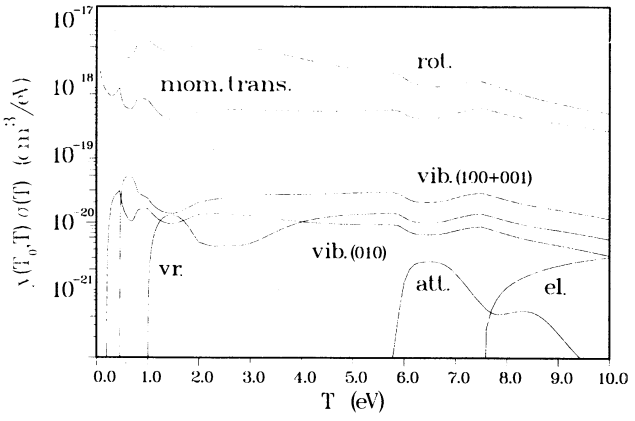

FIG. 5. Yield spectra in gaseous H_2O for the source energy $T_0=10$ eV. The ordinate represents the product of the degradation spectrum and the cross section for each process, and the abscissa represent the electron energy T. The area under the curve over any T interval corresponds to the contribution to the yield of each process from that interval per unit molecular density. The label "rot." represents rotational excitation, "mom. trans." the momentum transfer upon elastic scattering, "vib. (100+001)" the excitation of the 100 and 001 vibrational modes, "vib.(010)" the excitation of the 010 vibrational mode, "vr." the excitation of all the other vibrational modes, "att." the dissociative attachment, and "el." the electronic excitation.

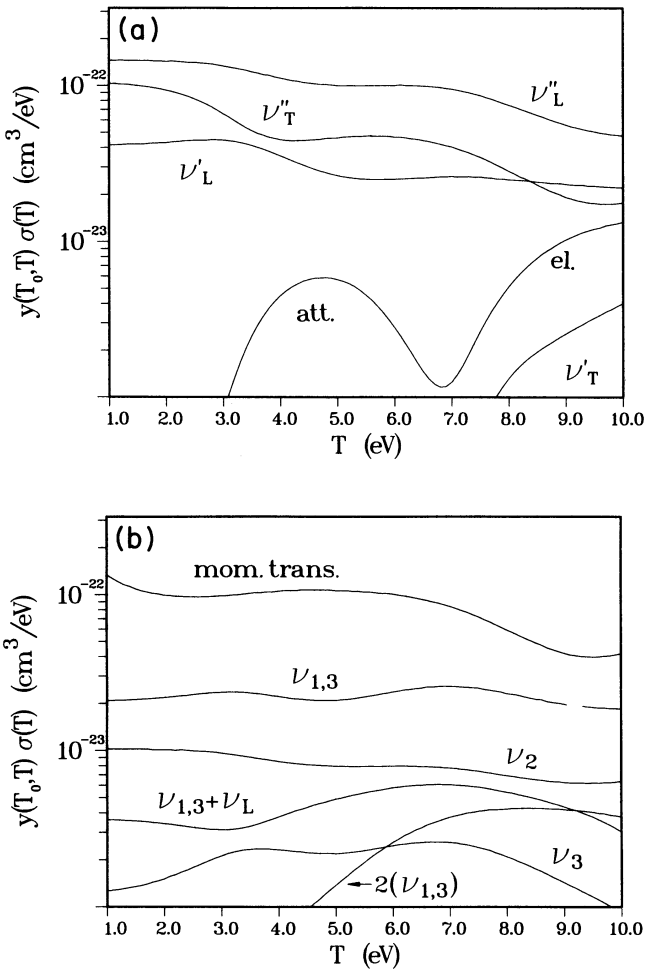

FIG. 6. Yield spectra in solid H_2O for the source energy $T_0=10$ eV. The ordinate represents the product of the degradation spectrum and the cross section for each process, and the abscissa represents the electron energy T. The area under the curve over any T interval corresponds to the contribution to the yield of each process from that interval per unit molecular density. In (a), symbols ν'_L and ν''_L represent two modes of libration (i.e., intermolecular vibration), ν'_T and ν''_T two modes of translational phonons. Label "el." represents electronic excitation. In (b) labels indicate various modes of intramolecular vibration.

through momentum transfer on elastic scattering) but is moderate in molecular gases (in which they do so through vibrational and rotational excitation as well). Thus the transition from the electronic-excitation region to the subexcitation region in a molecular gas is gradual.

Below about 7 eV the yield spectra for the vibrational excitation are roughly flat, signifying that subexcitation electrons at different energies contribute roughly equally to the yield of vibrational excitation. However, at energies below 2 eV, peaks in the yield spectra clearly reflect the structures of the vibrational-excitation cross sections seen in Fig. 1.

The yield spectrum for the rotational excitation shows a general rise with decreasing energy and structures below about 2 eV. These structures are out of phase

TABLE I. Yields of various processes in gaseous H_2O during electron degradation from the initial energy $T_0 = 10$ eV down to the terminal energy 0.06 eV.

Process	Methods	Yields	Difference between SF and CSDA (%)
Rotational excitation	SF	507	27
	CSDA	644	
Vibrational excitation			
(010)	SF	2.07	21
	CSDA	2.50	
(100+001)	SF	5.08	16
	CSDA	5.88	
Sum of remaining	SF	2.07	
excitations	CSDA	2.31	23
Electronic excitation	SF	0.179	28
	CSDA	0.129	
Attachment	SF	0.098	5
(H^- formation)	CSDA	0.103	

compared to the structures of the yield spectra for the vibrational excitation. For instance, at an electron energy where the yield spectrum for the vibrational excitation peaks, the yield spectrum for the rotational excitation is depressed. This interplay between the rotational excitation and the vibrational excitation was noted for nitrogen.[2]

B. Solid

Next we discuss the spectra in solid H_2O [Figs. 6(a) and 6(b)]. Going from the initial energy of 10 eV to the electronic-excitation threshold at 6.8 eV, we observe the rapid drop of the yield spectrum for the electronic excitation. The yield spectrum shows a hump between 3.5 and 6 eV with a maximum at 4.8 eV. The trends of these spectra are similar to those of the spectra in gaseous H_2O except for the shift in energy.

All the other yield spectra shown in Figs. 6(a) and 6(b) are roughly similar in shape to the corresponding cross sections shown in Figs. 2(a) and 2(b). This similarity arises from the mild energy dependence of the degradation spectrum in the CSDA, viz., the reciprocal of the stopping power. The yield spectra obtained from the SF

TABLE II. Yields of various processes in solid H_2O during electron degradation from the initial energy $T_0 = 10$ eV down to the terminal energy of 1 eV (referenced to the vacuum level).

Processes	Methods	Yields	Difference between SF and CSDA (%)
Phonon modes			
ν'_T	SF	0.523	64
	CSDA	0.188	
ν''_T	SF	18.9	28
	CSDA	13.7	
ν'_L	SF	11.5	25
	CSDA	8.63	
ν''_L	SF	37.1	25
	CSDA	28.0	
Vibrational modes			
ν_2 (bending)	SF	2.83	20
	CSDA	2.25	
$\nu_{1,3}$ (stretching)	SF	8.02	23
	CSDA	6.16	
ν_3	SF	0.623	12
	CSDA	0.548	
$\nu_{1,3}+\nu_L$	SF	1.44	15
	CSDA	1.23	
$2(\nu_{1,3})$	SF	0.939	37
	CSDA	0.589	
Electronic excitation	SF	1.40	50
	CSDA	0.699	
Electron attachment	SF	0.486	7
	CSDA	0.451	

degradation spectrum (not shown in the figures) are highly structured, but their mean behavior is roughly similar to the CSDA results.

VI. CSD TIME

Figures 7 and 8 show the CSD time, evaluated from Eq. (11), as a function of electron energy in gaseous and solid H_2O, respectively. Notice first the difference in the time scale of about 3 orders of magnitude between the gas and solid, which is obviously due to the difference in the molecular density. Apart from this, the following differences between Figs. 7 and 8 are noticeable. The downward curvature in the CSD time in the gas (Fig. 7) persists down to the lowest energies; this results from the increasing cross section for both momentum transfer and rotational excitation with decreasing energy (as seen in Fig. 1), which in turn results from the long-range dipole interactions of an electron with the H_2O molecule. In contrast, the behavior of the CSD time in the solid (Fig. 8) is almost linear on the logarithmic scale. This results from the virtual absence of rotational excitation in the solid.

VII. GROWTH OF YIELDS WITH THE CSD TIME

A general theory of the temporal evolution of the yield of a product was given by Inokuti, Kimura, and Dillon.[13] As a preliminary step before full application of the theory, we report here results of the CSDA. Within the CSDA, the cumulative yield $N_s(T_0;\tau)$ of a product s is given by

$$N_s(T_0;\tau)=n\int_{T(\tau)}^{T_0} d\lambda\, y(T_0,\lambda)\sigma_s(\lambda)\ , \tag{14}$$

where $T(\tau)$ signifies the energy T as a function of the CSD time τ as defined by Eq. (11) and the reciprocal of the stopping power replaces $y(T_0,\lambda)$.

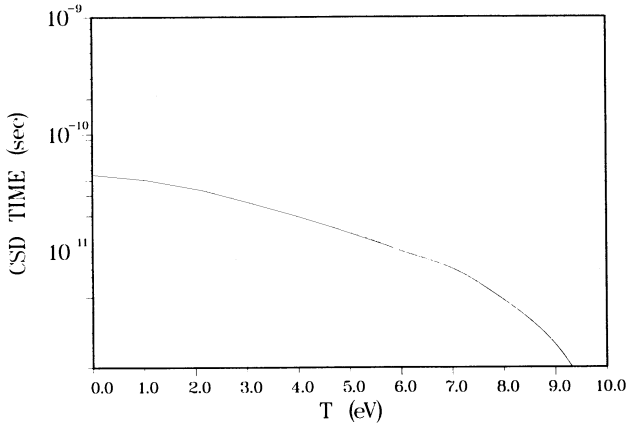

FIG. 7. The CSD time as a function of electron energy T in gaseous H_2O at pressure of 1 atm and temperature of 0 °C (the source energy $T_0=10$ eV). See Eq. (11) for the definition of CSD time.

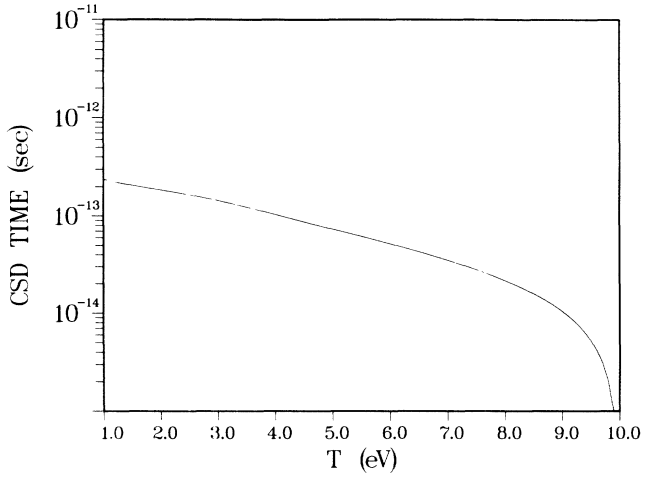

FIG. 8. The CSD time as a function of electron energy T in solid H_2O at 14 K (the source energy $T_0=10$ eV).

A. Gas

Figure 9 shows cumulative yields for various products in gas as functions of the CSD time.

The cumulative yields for dissociative attachment and

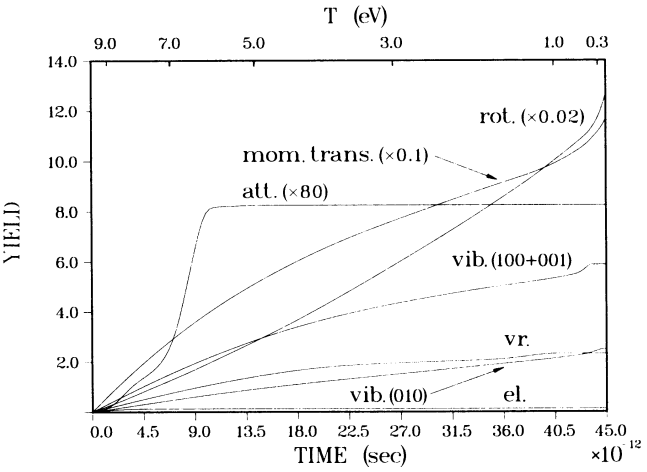

FIG. 9. Yields of various processes in gaseous H_2O as functions of the CSD time. The CSD time is evaluated from Eq. (11) for a pressure of 1 atm and a temperature of 0 °C and for the initial electron energy of 10 eV. The upper horizontal axis indicates the electron energy corresponding to the CSD time. The label "rot." represents the rotational excitation. The plotted value is the yield multiplied by 0.02. The label "mom. trans." represents the momentum transfer, and the symbol vib.(100+001) represents the excitation of the 100 and 001 vibrational modes, vib.(010) the excitation of the 010 vibrational mode, and vr. the excitation of all the other vibrational modes. The label "att." represents the dissociative attachment and "el." the electronic excitation. The figure shows the yield multiplied by 80 for the dissociative attachment.

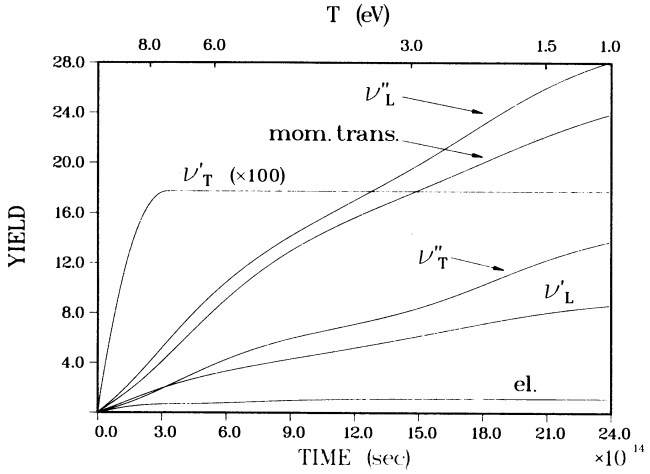

FIG. 10. Yields of various processes in solid H_2O as functions of the CSD time. The CSD time is evaluated from Eq. (11) for amorphous ice at 14 K and for the initial electron energy of 10 eV. The upper horizontal axis indicates the electron energy corresponding to the CSD time. The meanings of the labels are the same as in Fig. 6. For ν'_T, the plotted value is the yield multiplied by 100.

for electronic excitation rapidly rise and reach plateaus, which correspond to the yields under stationary irradiation (as seen in Table I). In other words, the dissociative attachment and the electronic excitation occur only at higher energies and therefore are completed by about 10^{-11} sec in the gas at 1 atm at 0 °C.

In contrast, the cumulative yields for the other products continue to grow in the time interval shown in Fig. 9. In particular, the cumulative yield for the rotational excitation rises steeply at $(40-45)\times10^{-12}$ s, when the mean energy of the electrons is about 1 eV. The same trend persists down to lower energies (not shown in the figure), until the electrons reach energies of about 0.02 eV. Thereafter, they begin to be thermalized. (Discussion of the electron thermalization process in this precise sense is outside the scope of the present paper.)

B. Solid

Figure 10 shows the cumulative yields for various products in solid H_2O. Again, the cumulative yields for electronic excitation and for ν'_T rapidly reach a plateau. All the other cumulative yields continue to grow throughout the time interval shown in the figure. We had to terminate calculations at 1 eV because of the absence of cross-section data.

VIII. TOTAL YIELDS OF PRODUCTS

Finally, we discuss the total yields of various products with the initial energy $T_0=10$ eV evaluated from Eq. (2). However, the meaning of the total yield must be qualified here. We have truncated the integral of Eq. (2) at a finite lower limit, which we may call the terminal energy. Its value is 0.06 eV in gas and 1 eV in solid, much higher than the thermal energy. The truncation is of no consequence for the yields of those processes with higher threshold energies such as the electronic excitation and the dissociative attachment. The terminal energy is critical to the yields of processes that have very low threshold energies, especially those with cross sections increasing with decreasing energy, such as rotational excitation in gas.

A. Gas

Table I shows results for gaseous H_2O. The yield of electronic excitation is low because we chose the initial energy as low as 10 eV. The yield of dissociative attachment is also modest because of the limited energy range, 5.8–7.5 eV, where the process occurs effectively, as seen from the yield spectrum (Fig. 5). This yield will increase only slightly if the initial energy is increased because electronic excitation dominates the energy loss at energies higher than 10 eV.

To obtain the radiation-chemical yield (G value), we must calculate $N_{att}(T_0)$ for various values of T_0 and take an average with respect to the entry spectrum[5,6] of subexcitation electrons. Although a full treatment is left for future work, it is instructive to make a rough estimate. On the assumption of the Platzman form[24] of the entry spectrum, the fraction of the subexcitation electrons produced in the relevant energy range, 5.8–7.5 eV, is about 0.23. Thus the yield of the dissociative attachment is about $0.23\times0.098=0.023$ per subexcitation electron, or per $W=29.6$ eV of absorbed energy.[25] Thus the yield is about 0.076 per 100 eV of absorbed energy.

The vibrational excitation has a high total yield for every channel. The sum of the yields for all the channels is about 9. As seen from the yield spectra (Fig. 5), the vibrational excitation occurs effectively at all energies down to the thresholds.

Table I also includes comparison between the CSDA and the SF solutions. For dissociative attachment, the total yields evaluated in the two ways agree within 5%. For all the other total yields, the discrepancies are larger. Comparison of the yield spectra indicates that the discrepancies arise mainly from the region, 8–10 eV, where the Lewis effect occurs in the SF solution. This also explains why the difference between the CSDA and the SF solutions is small for the dissociative attachment, which occurs chiefly at energies below the region of the Lewis effect.

B. Solid

Table II shows the total yields of various processes that occur in solid H_2O during the degradation of an electron from 10 to 1 eV.

The phonon excitation has a high yield for every mode except for the $\nu_{T'}$ mode, which occurs in competition with the electronic excitation. The sum of the yields for all the mode is 68. The vibrational excitation is less efficient, with a total yield of 13.8.

The electronic-excitation yield is modest because the initial energy T_0 is set at 10 eV; it will be much higher if T_0 is higher. The dissociative-attachment yield is appreciable with the value of 0.486 and is insensitive to T_0 so

long as T_0 is well above 6 eV.

The CSDA leads to considerably lower yields than the SF solution. The discrepancy in the solid is greater than in the gas. The discrepancy occurs because the structure in the SF degradation spectrum is especially prominent in the region (8–10 eV) of the Lewis effect and also persists down to 1 eV, as seen in Fig. 4.

IX. CONCLUDING REMARKS

As we saw in oxygen,[4] we find in H_2O that the degradation spectrum of the CSDA deviates largely from that of the SF and that yields are qualitatively and quantitatively different for the two treatments. The breakdown of the CSDA comes from in-phase structures of dominant vibrational cross sections in both phases. These characteristics of the cross sections enhance the Lewis effect and carry it over to lower energies.

Having seen the degradation spectra in gaseous and solid H_2O, one would naturally wonder about the electron degradation spectrum in liquid H_2O. In fact, a large portion of study in radiation chemistry has dealt extensively with water, mostly because of its importance in biology.[26] With regard to density, liquid H_2O is close to solid H_2O. As for the cross sections in liquid, most of the data presented in the literature concern the energy regime above the electronic-excitation threshold,[27] not the subexcitation regime. The most important cross sections in the subexcitation regime are the vibrational- and rotation-excitation cross sections. However, these cross sections have not been measured, and the results by Michaud and Sanche[8,9] for solid H_2O provide no guide to estimating these cross sections with confidence, especially the rotational-excitation cross section. A meaningful analysis of the degradation spectrum in the liquid phase at the level of the present treatment of gas and solid is currently impossible.

In the consideration of the differences among gas, solid, and liquid, the yield of the dissociative attachment is noteworthy. Our results are 0.075 for gas and 0.3 for solid, when expressed in terms of the G value, i.e., the yield per 100 eV of radiation energy absorbed. Platzman[19] gave 0.2 ± 0.1 for liquid, also expressed in terms of the G value. The three values are comparable and probably compatible among themselves. The yield in gas is based on the most reliable cross-section data. Its low value stems from the sharply peaked cross section as seen in Fig. 1 and also from rapid moderation, chiefly due to long-range dipole interactions, giving rise to the large momentum transfer and rotational-excitation cross sections. The yield in solid is higher because the cross section has broader peaks as seen in Fig. 2, and also probably because the rotational excitation is suppressed by strong intermolecular forces that are especially effective at 14 K. In liquid H_2O, the yield is intermediate because the dipolar energy losses are effective[28] and cause the electrons to degrade appreciably faster than in solid.

Lastly, the following remarks on the solid cross sections by Michaud and Sanche[8,9] are in order. Despite having different magnitudes, all cross sections for different processes show similar energy dependences in the entire energy region studied. Since these inelastic processes arise from different types of interactions between an electron and H_2O, one would naturally expect different energy dependences in their cross sections. For instance, vibrational excitations are due to the short-range interactions necessary to cause substantial transfer of energy between an incident electron and nuclear motion. Hence, vibrational-excitation cross sections in the gas and solid phases are expected to be similar in magnitude and shape. The trends of the reported cross sections[8,9] differ from this expectation. Perhaps this is due in part to the transport analysis used to extract the cross sections from the measured data. In this sense, the present study of the degradation spectrum for solid H_2O is considered to be still tentative. More experimental studies for determining the cross sections in the solid phase are desirable. In this respect, we suggest studies on solid D_2O, because it has larger quanta for vibrational modes and smaller quanta for librational modes than solid H_2O; the comparison between H_2O and D_2O should enable one to determine cross sections more precisely.

ACKNOWLEDGMENTS

This work was supported in part by the U.S. Department of Energy, Assistant Secretary for Energy Research, Office of Health and Environmental Research, under Contract No. W-31-109-Eng-38. We thank Leon Sanche, T. Goulet, and J. P. Jay-Gerin for discussions that led to our clearer understanding of their work than would otherwise have been possible.

*Also at Department of Physics, Rice University, Houston, TX 77251.

[1]M. A. Dillon, M. Inokuti, and M. Kimura, Radiat. Phys. Chem. **32**, 43 (1988).

[2]K. Kowari, M. Kimura, and M. Inokuti, J. Chem. Phys. **89**, 7229 (1988).

[3]A. Pagnamenta, M. Kimura, M. Inokuti, and K. Kowari, J. Chem. Phys. **89**, 6220 (1988).

[4]M. A. Ishii, M. Kimura, M. Inokuti, and K. Kowari, J. Chem. Phys. **90**, 3081 (1989).

[5]M. Inokuti, M. Kimura, and K. Kowari, Chem. Phys. Lett. **152**, 504 (1988).

[6]M. Kimura, M. Inokuti, and K. Kowari, Phys. Rev. A **40**, 2316 (1989).

[7]M. Inokuti, in *Molecular Processes in Space,* edited by T. Watanabe, I. Shimamura, M. Shimizu, and Y. Itikawa (Plenum, London, 1990), p. 65.

[8]M. Michaud and L. Sanche, Phys. Rev. A **36**, 4672 (1987).

[9]M. Michaud and L. Sanche, Phys. Rev. A **36**, 4684 (1987).

[10]T. Goulet and J.-P. Jay-Gerin, J. Phys. Chem. **92**, 6871 (1988).

[11]M. Hayashi, *Atomic and Molecular Data for Radiotherapy, Proceedings of an IAEA Advisory Group Meeting, Vienna, June 1988,* Report No. IAEA-TECDOC-506 (International Atomic Energy Agency, Vienna, 1989), p. 193.

[12]M. Inokuti, M. A. Dillon, and M. Kimura, Int. J. Quantum Chem. **21**, 251 (1987).
[13]M. Inokuti, M. Kimura, and M. A. Dillon, Phys. Rev. A **38**, 1217 (1988).
[14]T. W. Shyn, S. Y. Cho, and T. E. Cravens, Phys. Rev. A **38**, 678 (1988).
[15]Y. Itikawa, J. Phys. Soc. Jpn. **32**, 217 (1972).
[16]A. Jain and D. G. Thompson, J. Phys. B **16**, 3077 (1983).
[17]C. E. Melton and G. A. Neece, J. Am. Chem. Soc. **93**, 6757 (1971).
[18]C. E. Melton, J. Chem. Phys. **57**, 4218 (1972).
[19]R. L. Platzman (unpublished).
[20]H. W. Lewis, Phys. Rev. **135**, 937 (1962).
[21]D. A. Douthat, Radiat. Res. **61**, 1 (1975).
[22]K. Kowari and S. Sato, Bull. Chem. Soc. Jpn. **54**, 2878 (1981).
[22]K. Kowari and S. Sato, Bull. Chem. Soc. Jpn. **54**, 2878 (1981).
[23]K. Kowari, M. Kimura, and M. Inokuti, Phys. Rev. A **39**, 5545 (1989).
[24]R. L. Platzman, Radiat. Res. **2**, 1 (1955).
[25]International Commission on Radiation Units and Measurements, *Average Energy Required to Produce an Ion Pair,* ICRU Report No. 31 (International Commission on Radiation Units and Measurements, Washington, D.C., 1979), p. 28.
[26]See, for example, a recent review in this field, *Radiation Chemistry,* edited by Farhataziz and M. A. J. Rogers (VCH, New York, 1987), p. 137.
[27]H. G. Paretzke, in *Kinetics of Nonhomogeneous Processes,* edited by G. R. Freeman (Wiley, New York, 1987), p. 89.
[28]H. Fröhlich and R. L. Platzman, Phys. Rev. **92**, 1152 (1953).